Bulletin of the Geological Survey of Japan, vol. 68 (3), p. 119–130, 2017

Report

LA-ICP-MS U–Pb and fission-track ages of felsic tuff beds of the Takikubo Formation, Izumi Group in the Kan-onji district, eastern Shikoku, southwestern Japan

Atsushi Noda[1,*], Tohru Danhara[2], Hideki Iwano[2], and Takafumi Hirata[3]

Atsushi Noda, Tohru Danhara, Hideki Iwano and Takafumi Hirata (2017) LA-ICP-MS U–Pb and fission-track ages of felsic tuff beds of the Takikubo Formation, Izumi Group in the Kan-onji district, eastern Shikoku, southwestern Japan. *Bull. Geol. Surv. Japan*, vol. 68 (3), p. 119–130, 4 figs, 6 tables.

Abstract: LA-ICP-MS U–Pb and fission-track (FT) dating were performed for detrital zircons in two felsic tuff samples (KT01 and KT02) in order to estimate the depositional age of the Takikubo Formation (Izumi Group) in the Kan-onji district, eastern Shikoku, southwestern Japan. Total 30 grains analyzed for each sample indicated that the U–Pb ages composed of multiple populations chiefly of younger (75–85 Ma) and older (85–95 Ma) clusters. The concordia ages calculated by grains in the younger clusters were 78.3±0.5 Ma (2σ) for KT01 (number of accepted grains $n = 23$) and 80.8±0.7 Ma (2σ) for KT02 ($n = 9$). The U–Pb ages of KT01 are comparable with 79±7 Ma (2σ) of the FT age from the same sample. The U–Pb ages of KT01 could constrain the maximum depositional age near the basal part of the Takikubo Formation, which was middle of the Middle Campanian (polarity chron C33n in the magnetostratigraphy).

Keywords: Campanian, Cretaceous, Felsic tuff, Fission-track age, Izumi Group, Shikoku, Takikubo Formation, U–Pb age

1. Introduction

The Izumi Group is forearc basin deposits of the Late Cretaceous, which is narrowly distributed from western Shikoku to the Kii Peninsula along the northern side of the Median Tectonic Line. Macro-fossils (ammonoids and inoceramids) and micro-fossils (radiolarian assemblages) show that the depositional age of the Izumi Group are Campanian to Maastrichtian, Late Cretaceous (Suyari, 1973; Bando and Hashimoto, 1984; Yamasaki, 1987; Hashimoto *et al*., 2015). Those paleontological studies indicate that the depositional ages are younging toward the east. On the other hand, the paleocurrent directions in the main facies suggest the sediment derivation was mainly from east-northeast to west-southwest (Suyari, 1973; Miyata, 2004), as opposed to the younging direction of the depositional ages. These facts imply that the sedimentary basin of the Izumi Group had been developed in association with strike-slip fault activities (Ichikawa *et al*., 1981; Miyata, 1989; Noda and Toshimitsu, 2009). Progressive fault displacements along the pull-apart basins could migrate the basin depocenters (e.g., Noda, 2013).

Recently, details of the Late Cretaceous volcanic activities in the Sanyo Belt, which is situated at the north of the Izumi Group, were revealed by using U–Pb ages of igneous zircon grains in the felsic volcanic rocks and welded tuff beds (Sato, 2016; Sato *et al*., 2016a, b) (Fig. 1A). Therefore, radioisotope geochronological data in the Izumi Group may be useful to compare with the volcanic activities in magmatic fronts and to discuss temporal and spatial evolution of the sedimentary basin during the Late Cretaceous time. Although there are a few fission-track ages reported from the Izumi Group of Shikoku Island and the Kii Peninsula (Fig. 1A), no FT and U–Pb age data have been reported from eastern Shikoku to date.

This paper reports LA-ICP-MS U–Pb and FT ages of zircons in two felsic tuff beds of the Takikubo Formation (Yamasaki, 1986; Matsuura *et al*., 2002), which is the lower most formation of the main facies in the Izumi Group, eastern Shikoku. It is unclear whether or not the Takikubo Formation is an equivalent to the strata distributed in the Niihama district, central Shikoku (Fig. 1A). The depositional age of the Takikubo Formation was estimated to be of the lower Upper Campanian based on the radiolarian assemblages (Hashimoto *et al*., 2015; Noda and Kurihara, 2016).

[1] AIST, Geological Survey of Japan, Research Institute of Geology and Geoinformation
[2] Kyoto Fission-Track Co., Ltd.
[3] Division of Earth and Planetary Sciences, Kyoto University, Sakyo-ku, Kyoto 606-8502, Japan
Present address: Geochemical Research Center, Graduate School of Science, The University of Tokyo
[*] Corresponding author: A. Noda,Central 7,1-1-1 Higashi, Tsukuba, Ibaraki 305-8567, Japan. Email: a.noda@aist.go.jp

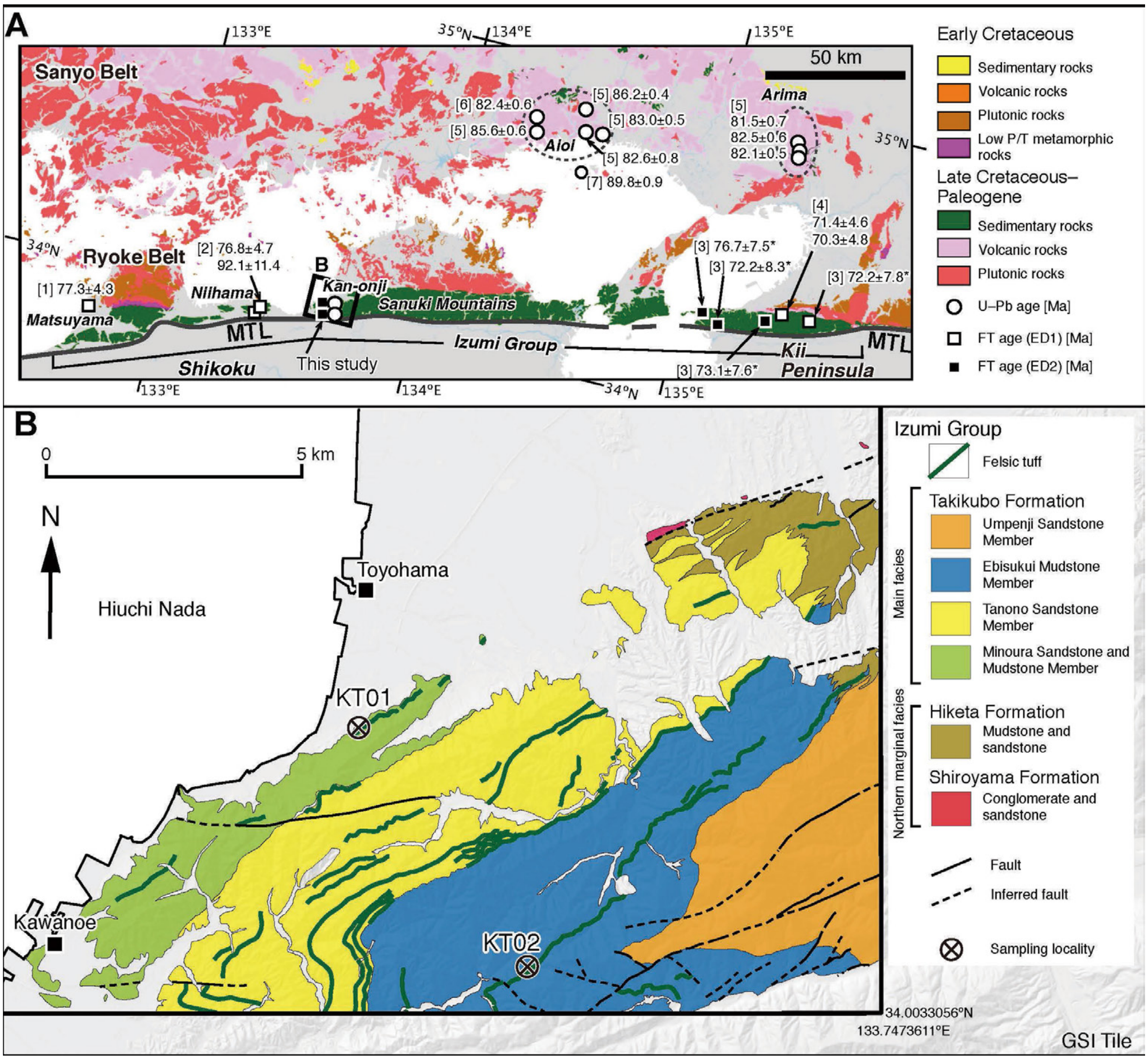

Fig. 1 A: Index map with U-Pb and fission-track (FT) ages (2σ) previously reported. FT ages include data obtained from the external detector method using internal surfaces (ED1) and external surfaces (ED2). The geological map is reproduced from the Seamless Digital Geological Map of Japan (Geological Survey of Japan, AIST, 2015). MTL means the Median Tectonic Line. References: [1] Sato *et al*. (2009), [2] Noda *et al*. (2010), [3] Miyata (2004), [4] Seike *et al*. (2013), [5] Sato *et al*. (2016a), [6] Sato *et al*. (2016b), and [7] Sato (2016). Asterisks (*) denote fission-track ages recalculated from the original data using the decay constant of $\lambda_D = 1.55125 \times 10^{-10}$ yr^{-1} instead of 1.480×10^{-10} yr^{-1}. B: Localities of felsic tuff samples (KT01 and KT02) for U-Pb and FT age analyses. Geological map of the Izumi Group is based on Noda *et al*. (in press). Shaded topography is from the GSI Maps (http://maps.gsi.go.jp/). Thick lines indicate the area of extent of the Kan-onji district.

2. Materials and methods

Two samples (KT01 and KT02) were obtained from felsic tuff beds in the Takikubo Formation of the Izumi Group, the western margin of the Sanuki Mountains (Fig. 1 and Table 1). The tuff bed of KT01 was intercalated within a mudstone-dominated sequence in the Minoura Sandstone and Mudstone Member which is the lowest member of the Takikubo Formation (Noda *et al*., in press). KT01 was collected from a very thick (more than 15 m in thick) felsic tuff bed composed of thin- to thick-bedded tuffaceous mudstones and siltstones with normal grading or parallel laminations (Fig. 2A). It was classified to vitric or crystal tuff showing light gray in color and silt- to fine sand-grained in size (Fig. 2B).

The sample KT02 was collected from a tuff bed in the Ebisukui Mudstone Member which is the third member of the Takikubo Formation. KT02 was obtained from a 7 m thick tuff bed which was composed of thin- to medium-bedded vitric tuff including fine- to coarse silt grains (Fig. 2C and D). The tuff bed included very fine sand-sized carbonaceous fragments parallel to the laminae. Although both samples of KT01 and KT02 were fine-grained, they contained euhedral to semi-euhedral zircon grains.

Table 1 List of samples analyzed. Longitude and latitude are based on WGS84 coordinate system.

Sample no.	ID	Longitude	Latitude	Date	Loc no.	Lithology	GSJ reg. no.
KT01	3499	133.63601	34.05375	2011-03-11	12	Felsic tuff	R108418
KT02	3287	133.67383	34.01164	2011-03-06	11	Felsic tuff	R108419

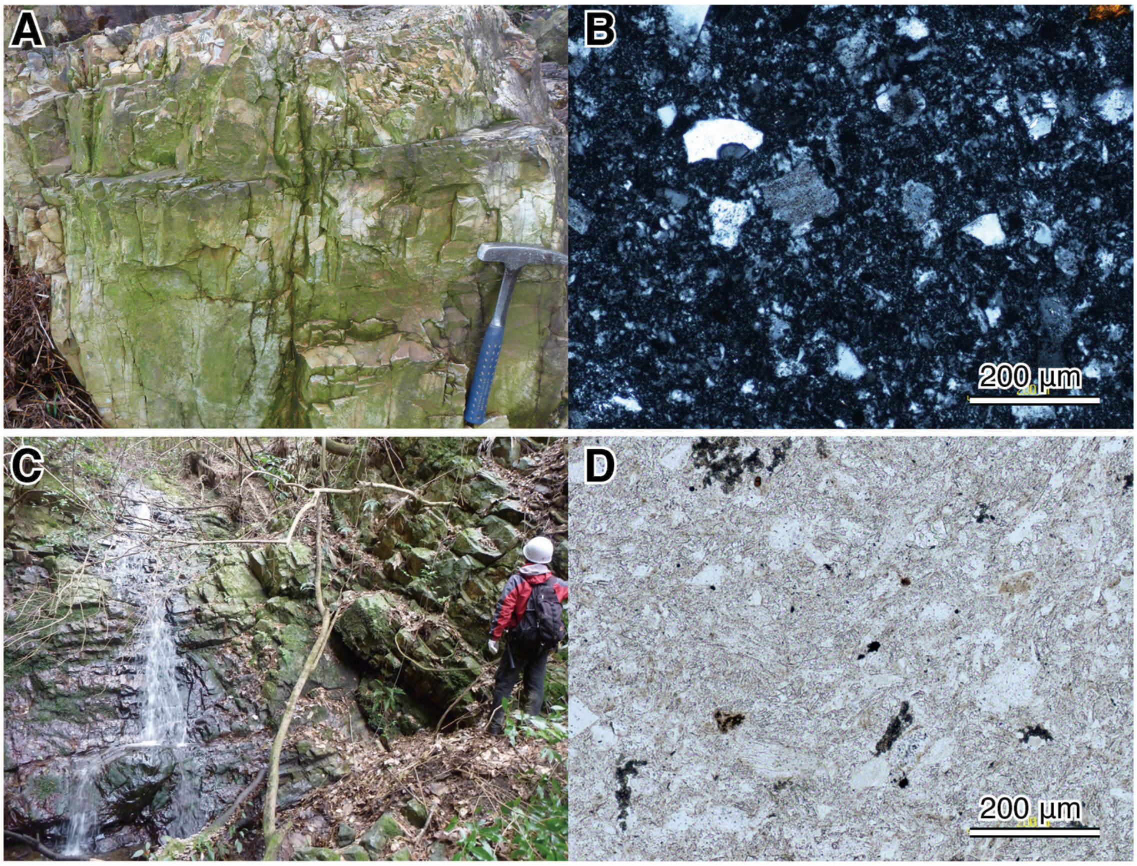

Fig. 2 A: Photograph of outcrop of the felsic tuff bed continued from the sampling locality of KT01. Wada, Toyohama-cho, Kan-onji, Kagawa. Length of the hammer is 33 cm. B: Photomicrograph of KT01 (crossed polar). C: Outcrop of KT02. Nakashita, Shimokawa-cho, Shikoku-Chuo, Ehime. D: Photomicrograph of KT02 (open polar).

The zircon grains were extracted from the samples; about 400 grains from 700 g for KT01 and 3,000 grains from 300 g for KT02. They were mounted on a PFA Teflon sheet with external natural surfaces exposed and etched by KOH–NaOH eutectic melts (KOH:NaOH = 1:1) at 225℃ during 19 hours. Because the zircon grains were very fine-grained, the measurements had to been conducted on the external surfaces of them instead of the internal ones. Spontaneous track density measurement was performed for 30 grains which were randomly selected using a high-resolution touch-monitor screen through a digital camera and an optical microscope (Danhara and Iwano, 2009).

U–Pb dating was performed on the same zircon grains with the track density counted ones by using LA- ICP-MS system installed in the Division of Earth and Planetary Science of Kyoto University, Japan (Table 2). The LA-ICP-MS system was a Nu Instruments (Wrexham, UK) AttoM high-resolution magnetic sector field ICP-MS (e.g., Yokoyama *et al*., 2011). The forward power of the ICP-MS was 1300 W (Iwano *et al*., 2013). Helium gas was used as the carrier gas inside the ablation cell and was mixed with argon gas before entering the ICP-MS. Signal intensities for ^{202}Hg, ^{204}(Pb+Hg), ^{206}Pb, ^{207}Pb, ^{232}Th, and ^{238}U were obtained from 30 zircon crystals on each sample. The laser ablation system was a New Wave Research NWR-193 ArF laser-ablation system (Fremont, CA 94538, USA; e.g., Sakata *et al*., 2014). The experimental conditions about the laser ablation include the wavelength (193 nm), the

Table 2 ICP-MS and laser operating conditions and data acquisition parameters.

Parameters	Value/Description
Laser ablation	
Model	New Wave Research NWR193
Laser type (Wave length)	Excimer ArF (193 nm)
Energy density	2.2 J/cm^2
Crater size	15 µm
Repetition rate	10 Hz
Carrier gas	He
ICP-MS	
Model	Nu Instruments AttoM
ICP-MS type	Magnetic sector field
Forward power	1300 W
Carrier gas	Ar
Ar gas flow rate	0.90 L min^{-1}
He gas flow rate	0.68 L min^{-1}
Scanning mode	Deflector jump
Data acquisition protocol	Batch
Integration time	8 s
Monitor isotopes	^{202}Hg, ^{204}Pb, ^{206}Pb, ^{207}Pb, ^{232}Th, ^{238}U
Primary standard	91500*1 (U-Pb), Fish Canyon Tuff*2 (FT)
Secondary standard	OD-3*3

*1 Wiedenbeck *et al*. (1995); *2 Danhara and Iwano (2013); *3 Iwano *et al*. (2013)

ablation pit size (15 µm), and the repetition rate (10 Hz).

The possible contribution of common Pb was monitored from ^{204}Pb signal with (or plus) ^{204}Hg as an isobaric interference. The abundance of ^{204}Hg was calculated from blank-corrected ^{202}Hg on the basis of the natural ^{202}Hg/^{204}Hg ratio, which in turn was subtracted from 204 total to yield ^{204}Pb. We applied one-shot cleaning on the sample surfaces before the analysis in order to reduce the risk of contamination of common Pb. Instrumental bias for the unknown ^{206}Pb*/^{238}U ratio (asterisk denotes radiogenic) was corrected using a 91500 zircon standard (Wiedenbeck *et al*., 1995).

The resultant U–Pb isotopic ratios and errors were used to calculate and plot concordia diagrams and histograms by Noda (2017). Details of the calculation for U–Pb ages and their errors are shown in Noda (2017). We excluded data whose error ellipses (2σ) do not overlap the concordia curves in the concordia diagrams as discordant data.

We also approximated FT ages for each grain by means of the ^{238}U signal data without internal standard correction based on Si or Zr. Age calibration was based on the zeta approach (Hurford, 1990a, b; Hasebe *et al*., 2013) using the age standard Fish Canyon Tuff with the absolute FT age being 28.4±0.2 Ma (Danhara and Iwano, 2013) and ζ = 44.0±6.0 for 91500 zircon as a uranium standard.

3. Results

3. 1 U–Pb ages

The ^{206}Pb*/^{238}U, ^{207}Pb*/^{235}U, and ^{207}Pb*/^{206}Pb* ages of zircons were calculated from analyzed isotopic ratios and decay constants.

KT01 The results of KT01 sample show a bimodal distribution whose ranges were roughly 75–85 Ma and 85–95 Ma; the younger population has a more conspicuous peak in the histogram (Fig. 3D; Table 3). We accepted grains whose error (3σ) of ^{206}Pb*/^{238}U ages includes the range of error (3σ) of the weighted mean of those in the younger cluster (Fig. 3C). By using the grains in the younger cluster (n = 23), the calculated ages are nearly consistent among the conventional concordia (^{207}Pb*/^{235}U–^{206}Pb*/^{238}U), Terra–Wasserburg concordia (^{238}U/^{206}Pb*–^{207}Pb*/^{206}Pb*), and the weighted mean of ^{206}Pb*/^{238}U ages, which are 78.3±0.5 Ma (2σ) of the concordia ages and 78.2±0.5 Ma (2σ) of the weighted mean of ^{206}Pb*/^{238}U ages (Fig. 3).

KT02 Most of the single grain ages in KT02 sample are concentrated in the older population of 85–95 Ma, but a small amount of grains are recognized within the younger one of 75–85 Ma (Fig. 4; Table 4). Because it is difficult to divide the clusters clearly by the dates, we chose grains in the same way as KT01 based on the error (3σ) of the weighted mean of ^{206}Pb*/^{238}U ages (Fig. 4C). The grains in this cluster (n = 9) yield 80.8±0.7 Ma (2σ) of the concordia ages (Fig. 4A and B) and 81.0±0.8 Ma (2σ) of the weighted mean of ^{206}Pb*/^{238}U ages (Fig. 4C). Because of the smaller numbers of accepted grains, these ages of KT02 show larger errors and MSWDs than those of KT01.

3. 2 FT ages

KT01 Individual FT ages were much more variable with larger errors than the U–Pb ages (Table 5). The weighted mean of the FT ages of 79±7 Ma (2σ), which was consistent with that of ^{206}Pb*/^{238}U age (78.2±0.5 Ma) of the same sample, was calculated with basically the same grains (n = 22) in the younger population of the U–Pb dating, except for one grain whose FT age was more than doubled the U–Pb age (Grain# 3 in Table 5).

KT02 The FT ages of zircon grains in the sample KT02 were also dispersed similar with KT01 (Table 6). The weighted mean of the FT ages was calculated by the selected grains (n = 8) in the younger population of the U–Pb age, except for one grain whose FT age was more than doubled the U–Pb age (Grain# 29 in Table 6). It was 69±10 Ma (2σ), which was younger than that of ^{206}Pb*/^{238}U ages (81.0±0.8 Ma) of the same sample.

4. Discussion

Because of the larger number of accepted grains and smaller errors and MSWDs, the U–Pb ages of KT01 are appropriate to constrain the maximum depositional age for the Minoura Sandstone and Mudstone Member in the Takikubo Formation. The lithology and sedimentary

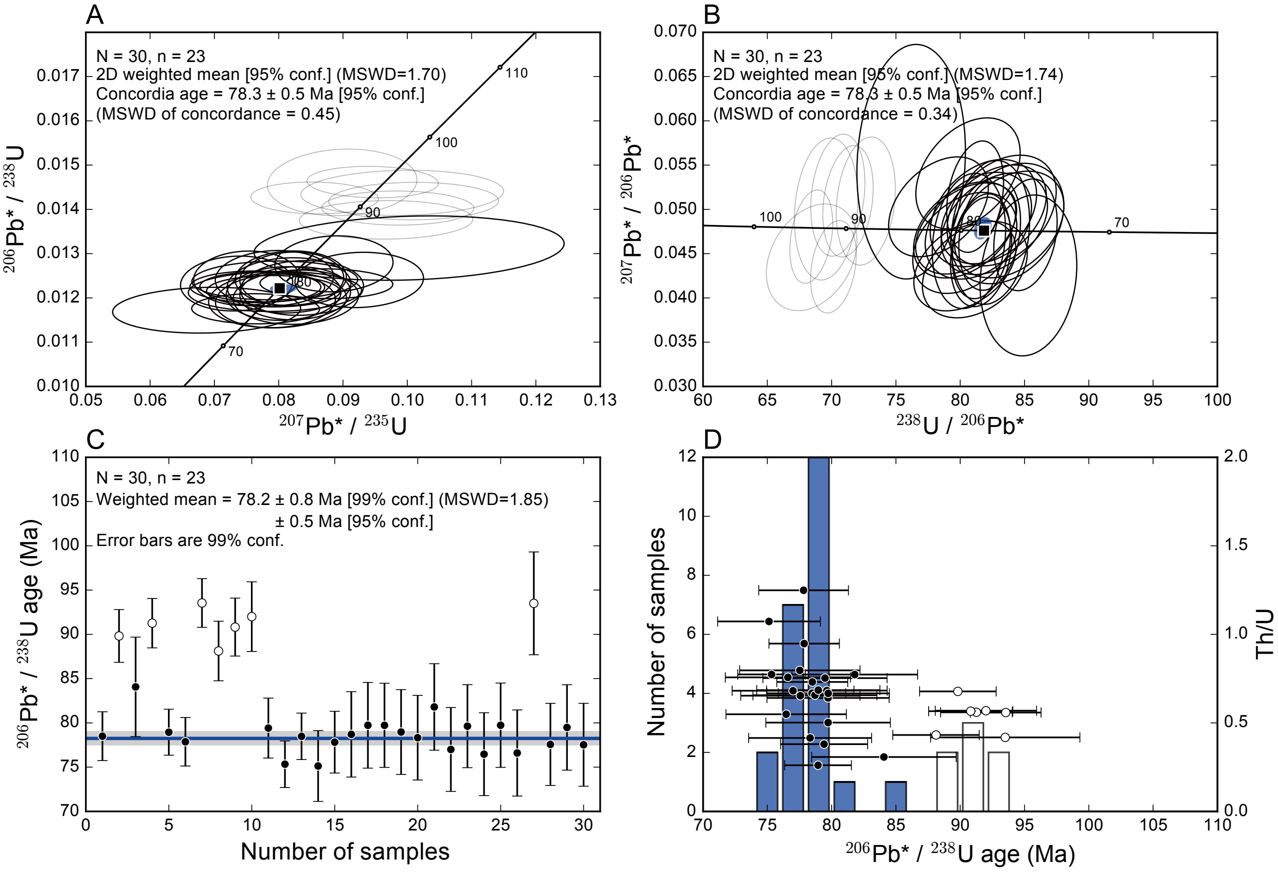

Fig. 3 Results of U–Pb dating of KT01. A: $^{207}Pb^{*}/^{235}U$–$^{206}Pb^{*}/^{238}U$ concordia diagram (Wetherill, 1956). Black solid and gray solid ellipses represent 2σ errors of accepted and excluded data points, respectively. Blue ellipse is a 95% confidence region of the two-dimensional weighted mean. Solid square shows the concordia age. *N* and *n* are numbers of total and accepted grains, respectively. B: Tera–Wasserburg concordia diagram (Tera and Wasserburg, 1972). Legends are same with A. C: one-dimensional weighted mean of $^{206}Pb^{*}/^{238}U$ ages (blue line) and its error of 3σ (gray band). Black and white circles with error bars (3σ) are accepted and excluded grains from the calculation, respectively. D: plots of Th/U ratios (right-hand vertical axis) with accepted (black circles) and excluded (white circles) data, and stacked histograms of $^{206}Pb^{*}/^{238}U$ ages (left-hand vertical axis) with accepted (blue bars) and excluded (white bars) data, respectively.

structures of the tuff beds, such as grading and parallel laminations, suggest the deposits were derived from volcaniclastic subaqueous gravity currents that transported pre-existing non-welded pyroclastic detritus from the land or shallow sea area (cf., Trofimovs *et al*., 2013). It means that the dates obtained from the zircon grains in the tuff beds do not indicate the depositional age directly. However, based on the very thick sediments in the Takikubo Formation (Noda *et al*., in press) and high productivity of pyroclastic detritus in the Sanyo Belt during this time (Sato *et al*., 2016a), it is probable that the zircon grains were transported from the source and deposited in the basin without a large time lag after the crystallization. Therefore, we approximate the depositional age of the Minoura Sandstone and Mudstone Member to 78.3±0.5 Ma (2σ) of the concordia ages or 78.2±0.5 Ma (2σ) of the weighted mean of $^{206}Pb{*}/^{238}U$ ages for the younger cluster in KT01, which corresponds to middle Middle Campanian and the polarity chron C33n in the magnetostratigraphy (Gradstein *et al*., 2012).

On the other hand, the U–Pb ages of KT02 from the Ebisukui Mudstone Member are older than those from KT01, although the tuff bed of KT02 is stratigraphically higher than that of KT01. Because tuff beds are considered to be not primary (pyroclastic) but secondary (volcaniclastic) deposits, the sample KT02 contained more recycled (older) grains. However, the depositional age of the Ebisukui Mudstone Member is at least younger than 80.8±0.7 Ma (2σ) based on the concordia ages of KT02.

FT ages of zircon grains are ideally equal to or younger than the U–Pb ages of them, if those crystals are supplied from volcanic eruptions. However, some FT ages in KT01 and KT02 show older ages than the U–Pb ages of the same grains. This discrepancy may be explained by two possibilities. The first is concentration of uranium measured in small spots (15 μm) by the LA-ICP-MS was

Table 3 Results of U–Pb age analysis of KT01. Asterisks (*) following the grain numbers mean excluded grains from calculation of concordia and weighted mean ages.

Sample KT01		Isotopic ratio						Discordance	Age [Ma]					
Grain#	Th/U	$^{207}Pb^*/^{206}Pb^*$	2σ	$^{206}Pb^*/^{238}U$	2σ	$^{207}Pb^*/^{235}U$	2σ	[%]	$^{206}Pb^*/^{238}U$	2σ	$^{207}Pb^*/^{235}U$	2σ	U [ppm]	Th [ppm]
1	0.73	0.0452	0.0050	0.01225	0.00029	0.0764	0.0082	concordant	78.5	1.9	74.7	8.3	269	197
2 *	0.68	0.0509	0.0051	0.01403	0.00031	0.0985	0.0095	concordant	89.8	2.0	95.4	9.6	276	187
3	0.31	0.0554	0.0107	0.01313	0.00058	0.1003	0.0194	concordant	84.1	3.8	97.0	19.5	56	17
4 *	0.56	0.0435	0.0042	0.01426	0.00029	0.0856	0.0080	concordant	91.3	1.9	83.4	8.1	345	193
5	0.26	0.0514	0.0051	0.01232	0.00027	0.0874	0.0083	concordant	78.9	1.7	85.1	8.4	321	84
6	0.95	0.0472	0.0051	0.01215	0.00029	0.0792	0.0084	concordant	77.9	1.8	77.4	8.4	270	256
7 *	0.56	0.0469	0.0042	0.01462	0.00029	0.0946	0.0082	concordant	93.5	1.8	91.8	8.3	379	212
8 *	0.43	0.0509	0.0058	0.01376	0.00035	0.0967	0.0109	concordant	88.1	2.3	93.7	11.0	193	83
9 *	0.57	0.0516	0.0055	0.01419	0.00034	0.1010	0.0106	concordant	90.8	2.2	97.7	10.7	218	123
10 *	0.57	0.0500	0.0065	0.01437	0.00041	0.0992	0.0127	concordant	92.0	2.6	96.0	12.8	139	79
11	0.38	0.0464	0.0061	0.01239	0.00035	0.0794	0.0104	concordant	79.4	2.3	77.6	10.5	163	62
12	0.77	0.0471	0.0051	0.01175	0.00027	0.0764	0.0080	concordant	75.3	1.8	74.8	8.1	285	220
13	0.67	0.0458	0.0048	0.01225	0.00027	0.0774	0.0078	concordant	78.5	1.8	75.7	7.9	309	206
14	1.07	0.0425	0.0073	0.01172	0.00042	0.0688	0.0118	concordant	75.1	2.7	67.5	11.9	103	110
15	1.25	0.0474	0.0065	0.01215	0.00036	0.0794	0.0108	concordant	77.8	2.3	77.6	10.9	148	184
16	0.66	0.0482	0.0049	0.01228	0.00050	0.0816	0.0077	concordant	78.7	3.2	79.6	7.8	272	179
17	0.50	0.0462	0.0046	0.01244	0.00050	0.0793	0.0074	concordant	79.7	3.2	77.5	7.5	289	145
18	0.64	0.0437	0.0041	0.01244	0.00049	0.0749	0.0066	concordant	79.7	3.2	73.4	6.7	347	222
19	0.69	0.0432	0.0044	0.01232	0.00050	0.0734	0.0070	concordant	79.0	3.2	72.0	7.1	296	203
20	0.41	0.0496	0.0049	0.01222	0.00050	0.0836	0.0077	concordant	78.3	3.2	81.5	7.8	283	117
21	0.77	0.0503	0.0045	0.01277	0.00051	0.0886	0.0074	concordant	81.8	3.3	86.2	7.5	329	255
22	0.68	0.0499	0.0050	0.01202	0.00049	0.0827	0.0078	concordant	77.0	3.2	80.6	7.9	268	183
23	0.68	0.0478	0.0041	0.01243	0.00049	0.0820	0.0065	concordant	79.6	3.1	80.1	6.6	395	269
24	0.55	0.0483	0.0048	0.01193	0.00049	0.0795	0.0075	concordant	76.5	3.1	77.7	7.6	282	155
25	0.67	0.0477	0.0044	0.01245	0.00050	0.0819	0.0070	concordant	79.7	3.2	79.9	7.0	342	228
26	0.76	0.0484	0.0055	0.01195	0.00051	0.0798	0.0086	concordant	76.6	3.3	78.0	8.7	212	161
27 *	0.42	0.0446	0.0048	0.01461	0.00060	0.0899	0.0094	concordant	93.5	3.9	87.4	9.5	206	86
28	0.65	0.0494	0.0045	0.01211	0.00048	0.0826	0.0069	concordant	77.6	3.1	80.5	7.0	348	227
29	0.75	0.0541	0.0050	0.01241	0.00050	0.0925	0.0080	concordant	79.5	3.2	89.9	8.1	291	219
30	0.80	0.0484	0.0046	0.01210	0.00049	0.0807	0.0072	concordant	77.5	3.1	78.8	7.3	314	250

Discordance is from $(1 - {}^{206}Pb^*/{}^{238}U\ age / {}^{207}Pb^*/{}^{235}U\ age) \times 100$.

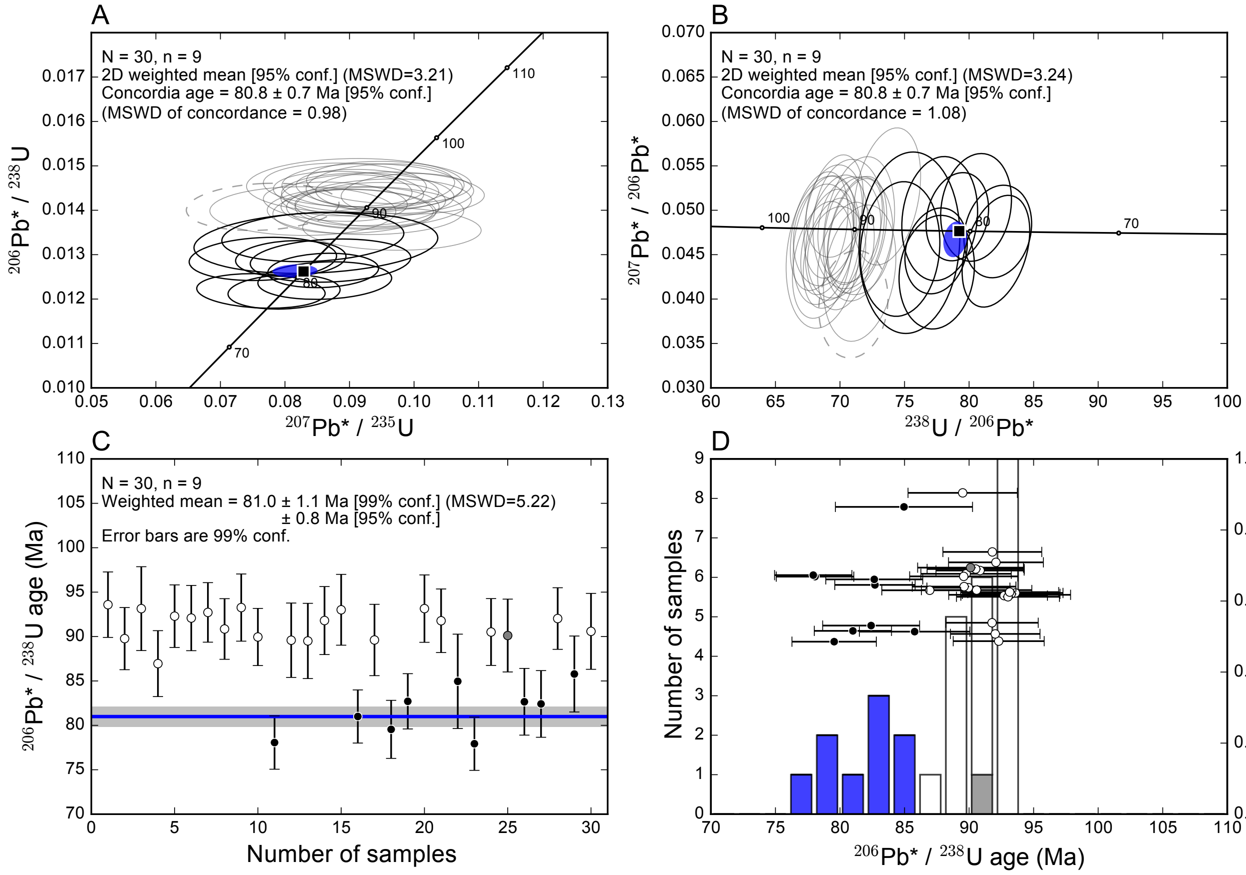

Fig. 4 Results of U–Pb dating of KT02. The discordant grain is represented by gray dashed ellipses (A and B), gray circle (C and D), and gray bar (D). Other legends are same with Fig. 3.

assumed to be the average concentrations of uranium in the grains. Because density of fission tracks in a grain depends on the average concentration of uranium in addition to duration of cooling, we might overestimate or underestimate the U concentrations for some grains. In the case of underestimation, apparent ages become older than the true ages, and vice versa.

The second is external effects of uranium outside or near the external surfaces of zircon grains, which mean contamination of fission-tracks originated from adjacent grains outside or enrichment of uranium along the external surfaces of the grains (Suzuki, 1988; Danhara *et al*., 1991). Because we used the external surfaces for the FT analysis, such effects might lead to older FT ages than the true ages.

5. Conclusions

The analyzed samples of KT01 (Minoura Sandstone and Mudstone Member) and KT02 (Ebisukui Mudstone Member) from tuff beds of the Takikubo Formation, Izumi Group, in the Kan-onji district contain multiple populations composed chiefly of younger (75–85 Ma) and older (85–95 Ma) ages. By using grains in the younger populations, the U–Pb ages of KT01 (n = 23) were 78.3±0.5 Ma (2σ) for the concordia ages and 78.2±0.5 Ma (2σ) for the weighted mean of ^{206}Pb*/^{238}U ages. Those of KT02 (n = 9) were 80.8±0.7 Ma (2σ) and 81.0±0.8 Ma (2σ), respectively. The FT ages were 79±7 Ma (2σ) for KT01 (n = 22) and 69±10 Ma (2σ) for KT02 (n = 8). Given intensive magmatisms during the Late Cretaceous in the Sanyo Belt, the depositional ages of the basal part of the Takikubo Formation could be constrained by the U–Pb ages of KT01, which is middle Middle Campanian, corresponding to the polarity chron C33n in the magnetostratigraphy.

Acknowledgements

Thin sections used in this study were prepared by Akira Owada, Takumi Sato, Kazuyuki Fukuda, and Eri Hirabayashi of the Geoinformation Service Center, Geological Survey of Japan, AIST. The early version of this manuscript was greatly improved by useful comments by reviewers of Yoshiaki Kon and Kazuhiro Miyazaki. This work is a part of the Geological Mapping Project supported by the Geological Survey of Japan, AIST.

Table 4 Results of U-Pb age analysis of KT02.

Sample KT02		Isotopic ratio						Discordance	Age [Ma]					
Grain#	Th/U	$^{207}Pb^{*}/^{206}Pb$	2σ	$^{206}Pb^{*}/^{238}U$	2σ	$^{207}Pb^{*}/^{235}U$	2σ	[%]	$^{206}Pb^{*}/^{238}U$	2σ	$^{207}Pb^{*}/^{235}U$	2σ	U [ppm]	Th [ppm]
1 *	0.62	0.0476	0.0054	0.01462	0.00038	0.0961	0.0103	concordant	93.6	2.5	93.2	10.4	226	141
2 *	0.68	0.0472	0.0053	0.01402	0.00036	0.0914	0.0097	concordant	89.8	2.3	88.8	9.8	245	166
3 *	0.62	0.0453	0.0069	0.01455	0.00049	0.0909	0.0136	concordant	93.1	3.2	88.3	13.7	103	63
4 *	0.63	0.0516	0.0062	0.01358	0.00039	0.0966	0.0111	concordant	87.0	2.5	93.6	11.2	184	116
5 *	0.49	0.0452	0.0050	0.01442	0.00037	0.0898	0.0094	concordant	92.3	2.4	87.4	9.5	258	126
6 *	0.71	0.0493	0.0056	0.01439	0.00038	0.0978	0.0105	concordant	92.1	2.5	94.8	10.6	220	156
7 *	0.62	0.0464	0.0048	0.01449	0.00035	0.0928	0.0089	concordant	92.7	2.3	90.1	9.0	322	198
8 *	0.69	0.0449	0.0049	0.01419	0.00036	0.0878	0.0090	concordant	90.9	2.3	85.5	9.1	280	192
9 *	0.62	0.0444	0.0053	0.01457	0.00039	0.0893	0.0102	concordant	93.3	2.5	86.8	10.3	204	127
10 *	0.64	0.0476	0.0048	0.01405	0.00033	0.0923	0.0086	concordant	90.0	2.2	89.6	8.7	350	223
11	0.67	0.0454	0.0051	0.01218	0.00031	0.0763	0.0080	concordant	78.1	2.0	74.6	8.1	296	198
12 *	0.67	0.0479	0.0065	0.01399	0.00044	0.0925	0.0122	concordant	89.6	2.8	89.8	12.4	134	90
13 *	0.90	0.0429	0.0062	0.01398	0.00044	0.0828	0.0116	concordant	89.5	2.8	80.7	11.7	130	118
14 *	0.74	0.0469	0.0057	0.01434	0.00040	0.0928	0.0107	concordant	91.8	2.6	90.1	10.9	188	139
15 *	0.61	0.0466	0.0058	0.01453	0.00042	0.0935	0.0112	concordant	93.0	2.7	90.8	11.3	170	104
16	0.52	0.0493	0.0040	0.01264	0.00031	0.0859	0.0069	concordant	81.0	2.0	83.7	7.0	651	336
17 *	0.64	0.0471	0.0053	0.01400	0.00042	0.0910	0.0104	concordant	89.6	2.7	88.4	10.5	207	132
18	0.49	0.0503	0.0049	0.01242	0.00034	0.0862	0.0083	concordant	79.5	2.2	83.9	8.4	344	167
19	0.65	0.0454	0.0039	0.01291	0.00032	0.0809	0.0069	concordant	82.7	2.1	79.0	7.0	556	359
20 *	0.63	0.0472	0.0046	0.01455	0.00040	0.0948	0.0093	concordant	93.1	2.5	92.0	9.4	307	192
21 *	0.54	0.0453	0.0041	0.01434	0.00037	0.0895	0.0082	concordant	91.8	2.4	87.1	8.3	398	214
22	0.86	0.0463	0.0082	0.01327	0.00055	0.0848	0.0152	concordant	85.0	3.6	82.6	15.3	75	65
23	0.67	0.0476	0.0042	0.01216	0.00031	0.0799	0.0070	concordant	77.9	2.0	78.0	7.1	511	344
24 *	0.69	0.0478	0.0048	0.01414	0.00039	0.0932	0.0094	concordant	90.5	2.5	90.5	9.5	285	197
25 *	0.69	0.0394	0.0049	0.01408	0.00043	0.0765	0.0095	–20.3	90.1	2.8	74.9	9.6	194	134
26	0.66	0.0430	0.0051	0.01290	0.00039	0.0766	0.0092	concordant	82.7	2.5	74.9	9.3	212	140
27	0.53	0.0491	0.0056	0.01287	0.00039	0.0871	0.0100	concordant	82.4	2.5	84.8	10.1	210	112
28 *	0.51	0.0499	0.0042	0.01438	0.00036	0.0990	0.0083	concordant	92.0	2.3	95.8	8.4	494	251
29	0.51	0.0456	0.0061	0.01340	0.00045	0.0843	0.0113	concordant	85.8	2.9	82.2	11.5	146	75
30 *	0.63	0.0485	0.0059	0.01415	0.00045	0.0946	0.0115	concordant	90.6	2.9	91.7	11.6	168	106

Discordance is from (1 – $^{206}Pb^{*}/^{238}U$ age/$^{207}Pb^{*}/^{235}U$ age) × 100.

Table 5 Preliminary results of fission-track dating of zircon samples in KT01 based on uranium data from LA-ICP-MS U–Pb dating.

Sample KT01	Fission Track Data			LA-ICP-MS-FT Age				
Grain#	N_s	A (10^{-6}cm^2)	ρ_s (10^6 cm^{-2})	U (ppm)	Age (Ma) t_{FT}		±2σ	
1	130	16.6	7.85	269	94	±	30	
2	51	5.5	9.24	276	108	±	42	*
3	87	14.7	5.91	56	336	±	117	**
4	53	5.5	9.60	345	90	±	35	*
5	45	7.4	6.11	322	62	±	25	
6	37	5.5	6.70	271	80	±	34	
7	111	8.3	13.41	380	114	±	38	*
8	49	7.4	6.66	194	111	±	44	*
9	59	5.5	10.69	218	158	±	60	*
10	22	5.5	3.99	140	92	±	47	*
11	94	16.6	5.68	163	112	±	38	
12	37	5.5	6.70	285	76	±	33	
13	79	9.2	8.59	309	90	±	32	
14	41	9.2	4.46	103	139	±	58	
15	42	11.0	3.80	148	83	±	34	
16	35	3.7	9.51	277	111	±	48	
17	43	5.5	7.79	295	86	±	35	
18	106	9.2	11.52	353	105	±	35	
19	44	6.4	6.83	302	73	±	30	
20	45	7.4	6.11	288	69	±	28	
21	49	7.4	6.66	336	64	±	25	
22	47	4.6	10.22	273	121	±	48	
23	54	7.4	7.34	402	59	±	23	
24	23	3.7	6.25	287	71	±	35	
25	44	5.5	7.97	348	74	±	30	
26	12	1.8	6.52	216	98	±	63	
27	47	8.3	5.68	209	88	±	35	*
28	33	3.7	8.97	354	82	±	36	
29	28	3.7	7.61	296	83	±	39	
30	31	4.6	6.74	319	68	±	31	
			Weighted mean (n = 22):		**79**	±	**7**	

N_s Number of spontaneous fission tracks counted
A Counting area
ρ_s Spontaneous track density (= N_s/A)
U Uranium concentration in ppm
FT age $t_{FT} = (1/\lambda_D)\ln(1+\lambda_D\zeta_{MS}g\rho_s/m_i)$ (see Hasebe *et al.*, 2013)
λ_D: Total decay constant of ^{238}U (= 1.55125×10^{-10} y^{-1})
ζ_{MS}: Zeta calibration factor determined by LA-ICP-MS
$\zeta_{MS} \pm 1\sigma = 44.0 \pm 6.0$
g: Geometry factor (=1)
$m_i = (^{238}U/^{29}Si)_{sample}/(^{238}U/^{29}Si)_{standard}$ for zircon grain *i*
$^{29}Si_{sample} = ^{29}Si_{91500\ standard}$ was supposed.
The count-area-corrected ^{238}U signal intensity was used.
Age standard Fish Canyon Tuff (28.4±0.2 Ma: Danhara and Iwano, 2013)
Uranium standard Nancy 91500, 74 ppm U
* Rejected data by U–Pb dating
** Manually excluded datum as an outlier

Table 6 Preliminary results of fission-track dating of zircon samples in KT02 based on uranium data from LA-ICP-MS U–Pb dating.

	Fission Track Data			LA-ICP-MS-FT Age				
Sample KT02	N_s	A	ρ_s	U	Age (Ma)			
Grain#		($10^{-6}cm^2$)	(10^6 cm^{-2})	(ppm)	t_{FT}		±2σ	
1	88	9.2	9.57	231	134	±	46	*
2	131	16.6	7.91	250	102	±	33	*
3	41	7.4	5.57	105	171	±	71	*
4	30	5.5	5.43	188	94	±	43	*
5	24	3.7	6.52	263	80	±	39	*
6	41	5.5	7.43	224	107	±	44	*
7	244	27.6	8.84	329	87	±	26	*
8	103	8.3	12.44	285	141	±	47	*
9	83	8.3	10.02	208	155	±	54	*
10	97	7.4	13.18	357	119	±	41	*
11	47	5.5	8.51	302	91	±	37	
12	20	3.7	5.43	137	128	±	67	*
13	33	3.7	8.97	133	217	±	97	*
14	40	5.5	7.25	192	122	±	51	*
15	28	5.5	5.07	173	95	±	44	*
16	74	5.5	13.41	645	67	±	24	
17	41	7.4	5.57	205	88	±	37	*
18	44	5.5	7.97	341	76	±	31	
19	74	7.4	10.05	551	59	±	21	
20	28	2.8	10.14	303	108	±	51	*
21	109	9.2	11.85	394	97	±	32	*
22	16	5.5	2.90	74	126	±	72	
23	127	13.8	9.20	506	59	±	19	
24	73	11.0	6.61	282	76	±	27	*
25	51	5.5	9.24	192	155	±	61	*
26	39	7.4	5.30	210	82	±	34	
27	38	7.4	5.16	208	80	±	34	
28	36	3.7	9.78	489	65	±	28	*
29	74	8.3	8.94	144	199	±	71	**
30	61	8.3	7.37	166	143	±	54	*
			Weighted mean (n = 8):		**69**	±	**10**	

N_s Number of spontaneous fission tracks counted
A Counting area
ρ_s Spontaneous track density (= N_s/A)
U Uranium concentration in ppm
FT age $t_{FT} = (1/\lambda_D)\ln(1+\lambda_D\zeta_{MS}g\rho_s/m_i)$ (see Hasebe *et al*., 2013)
λ_D: Total decay constant of ^{238}U (= 1.55125×10^{-10} y^{-1})
ζ_{MS}: Zeta calibration factor determined by LA-ICP-MS
$\zeta_{MS} \pm 1\sigma = 44.0 \pm 6.0$
g: Geometry factor (=1)
$m_i = (^{238}U/^{29}Si)_{sample}/(^{238}U/^{29}Si)_{standard}$ for zircon grain i
$^{29}Si_{sample} = {}^{29}Si_{91500\ standard}$ was supposed.
The count-area-corrected ^{238}U signal intensity was used.
Age standard Fish Canyon Tuff (28.4±0.2 Ma: Danhara and Iwano, 2013)
Uranium standard Nancy 91500, 74 ppm U
* Rejected data by U–Pb dating
** Manually excluded datum as an outlier

References

Bando, Y. and Hashimoto, H. (1984) Biostratigraphy and ammonite fauna of the Izumi Group (Late Cretaceous) in the Asan Mountains. *Mem. Fac. Educ., Kagawa Univ., Part II*, **34**, 1–16, (in Japanese with English abstract).

Danhara, T. and Iwano, H. (2009) Determination of zeta values for fission-track age calibration using thermal neutron irradiation at the JRR-3 reactor of JAEA, Japan. *Jour. Geol. Soc. Japan*, **115**, 141–145.

Danhara, T. and Iwano, H. (2013) A review of the present state of the absolute calibration for zircon fission track geochronometry using the external detector method. *Island Arc*, **22**, 264–279.

Danhara, T., Kasuya, M., Iwano, H. and Yamashita, T. (1991) Fission-track age calibration using internal and external surfaces of zircon. *Jour. Geol. Soc. Japan*, **97**, 977–985.

Geological Survey of Japan, AIST ed. (2015) *Seamless digital geological map of Japan 1:200,000, May 29, 2015 version*, Geol. Surv. Japan, AIST, (accessed 2016-05-29).

Gradstein, F. M., Ogg, J. G., Schmitz, M. D. and Ogg, G. M. eds. (2012) *The Geologic Time Scale*, Elsevier, Amsterdam, Netherland, 1144p.

Hasebe, N., Tamura, A. and Arai, S. (2013) Zeta equivalent fission-track dating using LA-ICP-MS and examples with simultaneous U–Pb dating. *Island Arc*, **22**, 280–291.

Hashimoto, H., Ishida, K., Yamasaki, T., Tsujino, Y. and Kozai, T. (2015) Revised radiolarian zonation of the Upper Cretaceous Izumi inter-arc basin (SW Japan). *Rev. Micropaléontol.*, **58**, 29–50.

Hurford, A. J. (1990a) International union of geological sciences subcommission on geochronology recommendation for the standardization of fission track dating calibration and data reporting. I*nt. Jour. Radiat. Appl. Instrum. Part D.*, **17**, 233–236.

Hurford, A. J. (1990b) Standardization of fission track dating calibration; recommendation by the Fission Track Working Group of the I.U.G.S. Subcommission on Geochronology. *Chem. Geol.*, **80**, 171–178.

Ichikawa, K., Miyata, T. and Shinohara, M. (1981) Eastward stepwise shift of the Izumi sedimentary basin with reference to the movement picture of the Median Tectonic Line. *In Proceedings of the Kansai Branch*, 11–12, Geol. Soc. Japan, (in Japanese).

Iwano, H., Orihashi, Y., Hirata, T., Ogasawara, M., Danhara, T., Horie, K., Hasebe, N., Sueoka, S., Tamura, A., Hayasaka, Y., Katsube, A., Ito, H., Tani, K., Kimura, J.-I., Chang, Q., Kouchi, Y., Haruta, Y. and Yamamoto, K. (2013) An inter-laboratory evaluation of OD-3 zircon for use as a secondary U–Pb dating standard. *Island Arc*, **22** 382–394.

Matsuura, H., Kurimoto, C., Yoshida, F., Saito, Y., Makimoto, H., Toshimitsu, S., Iwaya, T., Komazawa, M. and Hiroshima, T. (2002) *Okayama and Marugame*, Geological Map of Japan 1:200,000, Geol. Surv. Japan, AIST, Tsukuba, Japan.

Miyata, T. (1989) Cretaceous Izumi sedimentary basin: Pullaparts with duplex structure along Median Tectonic Line, southwest Japan. *In Abstracts*, the 28th International Geological Congress, Washington, DC, United States, p. 447.

Miyata, T. (2004) The Upper Cretaceous Izumi Group. *In Geology of the Kokawa district*, Quadrangle Series, 1:50,000, Geol. Surv. Japan, AIST, 28–40, (in Japanese).

Noda, A. (2013) Strike-slip basin: Its configuration and sedimentary facies. *In* Itoh, Y. ed. *Mechanism of Sedimentary Basin Formation: Multidisciplinary Approach on Active Plate Margins*, InTech, Rijeka, Croatia, 28–57, doi: 10.5772/56593.

Noda, A. (2017) A new tool for calculation and visualization of U–Pb age data: UPbplot.py. *Bull. Geol. Surv. Japan.*, **68**, 131–140.

Noda, A. and Kurihara, T. (2016) Late Cretaceous radiolarian assemblages obtained from the Izumi Group in the Kan-onji district, eastern Shikoku, Japan. *Bull. Geol. Surv. Japan*, **67**, 119–131 (in Japanese with English abstract).

Noda, A. and Toshimitsu, S. (2009) Backward stacking of submarine channel-fan successions controlled by strike-slip faulting: The Izumi Group (Cretaceous), southwest Japan. *Lithosphere*, **1**, 41–59.

Noda, A., Toshimitsu, S., Kurihara, T., and Iwano, H. (2010) Stratigraphy and depositional age of the Izumi Group, Niihama area, central Shikoku, Japan. *Jour. Geol. Soc. Japan*, **116**, 99–113, (in Japanese with English abstract).

Noda, A., Ueki, T., Kawabata, H., Matsuura, H. and Aoya, M. (in press) *Geology of Kan-onji district*, Quadrangle Series, 1:50,000, Geol. Surv. Japan, AIST, (in Japanese with English abstract).

Sakata, S., Hattori, K., Iwano, H., Yokoyama, T. D., Danhara, T. and Hirata, T. (2014) Determination of U–Pb ages for young zircons using Laser Ablation-ICP-Mass Spectrometry coupled with an ion detection attenuator device. *Geostand. Geoanal. Res.*, **38**, 409–420.

Sato, D. (2016) Zircon U–Pb and fission-track ages of Late Cretaceous volcanic rocks of the Ieshima Islands, southwest Japan. *Japan. Mag. Mineral. Petrol. Sci.*, **45**, 53–61, (in Japanese with English abstract).

Sato, D., Matsuura, H. and Yamamoto, T. (2016a) Timing of the Late Cretaceous ignimbrite flare-up at the eastern margin of the Eurasian Plate: New zircon U–Pb ages from the Aioi–Arima–Koto region of SW Japan. *Jour. Volcanol. Geotherm. Res.*, **310**, 89–97.

Sato, D., Yamamoto, T. and Takagi, T. (2016b) *Geology of the Banshu-Ako district*, Quadrangle Series, 1:50,000, Geol. Surv. Japan, AIST, 68p. (in Japanese with English abstract, 3p).

Sato, T., Kitagawa, Y., Koizumi, N., Natori, J., NIshimura, Y., Haga, M., Hirooka, S. and Tanikawa, S. (2009) *Geological data of the GSJ boring core at the Matsuyama Observation Station*, Open-File Report, no. 504, Geol. Surv. Japan, AIST, (in Japanese).

Seike, K., Iwano, H., Danhara, T. and Hirano, H. (2013) Tectonics of the Ryoke–Izumi belt of the Izumi Mountains, Southwest Japan from thermochronological data. *Jour. Geol. Soc. Japan*, **119**, 759–775, (in Japanese with English abstract).

Suyari, K. (1973) On the lithofacies and the correlation of the Izumi Group of the Asan Mountain Range, Shikoku. *Sci. Rep. Tohoku Univ., 2nd ser. (Geol.), Special Volume*, **6**, 489–495, (in Japanese with English abstract).

Suzuki, K. (1988) Heterogeneous distribution of Uranium within zircon grains: Implication for fission-track dating. *Jour. Geol. Soc. Japan*, **94**, 1–10.

Tera, F. and Wasserburg, G. J. (1972) U-Th-Pb systematics in three Apollo 14 basalts and the problem of initial Pb in lunar rocks. *Earth Planet. Sci. Lett.*, **14**, 281–304.

Trofimovs, J., Talling, P. J., Fisher, J. K., Sparks, R. S. J., Watt, S. F. L., Hart, M. B., Smart, C. W., Le Friant, A., Cassidy, M., Moreton, S. G. and Leng, M. J. (2013) Timing, origin and emplacement dynamics of mass flows offshore of SE Montserrat in the last 110 ka: Implications for landslide and tsunami hazards, eruption history, and volcanic island evolution. *Geochem. Geophys. Geosyst.*, **14**, 385–406.

Wetherill, G. W. (1956) Discordant uranium-lead ages, I. *Eos, Trans. Amer. Geophys. Union*, **37**, 320–326.

Wiedenbeck, M., Allé, P., Corfu, F., Griffin, W. L., Meier, M., Oberli, F., Quadt, A. V., Roddick, J. C. and Spiegel, W. (1995) Three natural zircon standards for U-Th-Pb, Lu-Hf, trace element and REE analyses. *Geostand. Newsl.*, **19**, 1–23.

Yamasaki, T. (1986) Sedimentological study of the Izumi Group in the northern part of Shikoku, Japan. *Sci. Rep. Tohoku Univ., 2nd ser. (Geol.)*, **56**, 43–70.

Yamasaki, T. (1987) Radiolarian assemblages of the Izumi Group in Shikoku and western Awaji Island, Southwest Japan. *Jour. Geol. Soc. Japan*, **93**, 403–417, (in Japanese with English abstract).

Yokoyama, T. D., Suzuki, T., Kon, Y. and Hirata, T. (2011) Determinations of rare earth element abundance and U-Pb age of zircons using multispot Laser Ablation-Inductively Coupled Plasma Mass Spectrometry. *Anal. Chem.*, **83**, 8892–8899.

Recieved April 28, 2016
Accepted January 23, 2017

四国東部の観音寺地域に分布する和泉層群滝久保層の珪長質凝灰岩の LA-ICP-MS による U–Pb 年代とフィッション・トラック年代

野田　篤・檀原　徹・岩野英樹・平田岳史

要　旨

四国東部の観音寺地域に分布する和泉層群滝久保層の堆積年代を推定するために，挟在する珪長質凝灰岩の2試料（KT01とKT02）について，LA-ICP-MSによる砕屑性ジルコン粒子のU-Pb年代とフィッション・トラック（FT）年代を測定した．各試料について，それぞれ30粒子を測定した結果，その年代分布は主に若い年代集団（75–85 Ma）と古い年代集団（85–95 Ma）から構成されることが分かった．若い年代集団に基づくコンコーディア年代は，KT01（採用粒子数n＝23）では78.3±0.5 Ma（2σ），KT02（n = 9）では 80.8±0.7 Ma（2σ）であった．また，KT01のU-Pb年代は，同じ粒子による79±7 Ma（2σ）のFT年代とほぼ一致する．これらの結果から推定される滝久保層の堆積年代は，後期白亜紀の中期カンパニアン期の中頃（古地磁気極性 C33n）である．